Available at www.sciencedirect.com

ScienceDirect

journal homepage: www.elsevier.com/locate/watres

Fouling behavior of microstructured hollow fiber membranes in submerged and aerated filtrations

P.Z. Çulfaz [a,c], M. Wessling [b,c], R.G.H. Lammertink [a,*]

[a] Soft Matter, Fluidics and Interfaces, MESA+ Institute for Nanotechnology, University of Twente, P.O. Box 217, 7500 AE Enschede, The Netherlands

[b] Chemical Process Engineering, AVT, RWTH Aachen University, Turmstr. 46, 52056 Aachen, Germany

[c] Membrane Technology Group, University of Twente, P.O. Box 217, 7500 AE Enschede, The Netherlands

ARTICLE INFO

Article history:
Received 17 October 2010
Received in revised form
28 November 2010
Accepted 4 December 2010
Available online 10 December 2010

Keywords:
Microstructured membrane
MBR
Fouling
Concentration polarization
Bubble flow

ABSTRACT

The performance of microstructured hollow fiber membranes in submerged and aerated systems was investigated using colloidal silica as a model foulant. The microstructured fibers were compared to round fibers and to twisted microstructured fibers in flux-stepping experiments. The fouling resistances in the structured fibers were found to be higher than those of round fibers. This was attributed to stagnant zones in the grooves of the structured fibers. As the bubble sizes were larger than the size of the grooves of the structured fibers, it is possible that neither the bubbles nor the secondary flow caused by the bubbles can reach the bottom parts of the grooves. Twisting the structured fibers around their axes resulted in decreased fouling resistances. Large, cap-shaped bubbles and slugs were found to be the most effective in fouling removal, while small bubbles of sizes similar to the convolutions in the structured fiber did not cause an improvement in these fibers. Modules in a vertical orientation performed better than horizontal modules when coarse bubbling was used. For small bubbles, the difference between vertical and horizontal modules was not significant. When the structured and twisted fibers were compared to round fibers with respect to the permeate flowrate produced per fiber length instead of the actual flux through the convoluted membrane area, they showed lower fouling resistance than round fibers. This is because the enhancement in surface area is more than the increase in resistance caused by stagnant zones in the grooves of the structured fibers. From a practical point of view, although the microstructure does not promote further turbulence in submerged and aerated systems, it can still be possible to enhance productivity per module with the microstructured fibers due to their high surface area-to-volume ratio.

1. Introduction

Membrane bioreactor (MBR) technology, which combines the activated sludge process in wastewater treatment with membrane separation, offers an attractive alternative for the conventional wastewater treatment process (Shannon et al., 2008; Buer and Cumin, 2010; Judd, 2008). The most important advantages offered by MBRs are smaller footprint, high product quality and lower waste production (Ho and Zydney, 2006; Le-Clech et al., 2006; Melin et al., 2006; Meng et al., 2009). Although the MBR process has found widespread use in wastewater treatment in the recent years, performance decline due to membrane fouling still remains the biggest challenge facing further development and application of this

* Corresponding author.
E-mail address: r.g.h.lammertink@utwente.nl (R.G.H. Lammertink).
0043-1354/$ – see front matter © 2010 Elsevier Ltd. All rights reserved.
doi:10.1016/j.watres.2010.12.007

technology (Ho and Zydney, 2006; Le-Clech et al., 2006; Meng et al., 2009).

In membrane bioreactors, air bubbles which are supplied to the reactor to provide dissolved oxygen for the microorganisms and to maintain the solids in suspension also serve the purpose of reducing fouling. This is due to the shear created on the surface of the membranes as a result of the liquid flow caused by bubbles, the scouring action of the bubbles themselves, the secondary flows they induce in the liquid and the fiber movement induced by the passing bubbles (Cui et al., 2003). Although aeration is a very effective way of reducing fouling, it also forms the main component of the operating costs (Judd, 2008; Le-Clech et al., 2006; Sofia et al., 2004). Periodic backwashing or intermittent operation, which serves to relax the cake layer on the membranes during the time permeation is stopped, are other ways of preventing fouling. However both decrease the amount of permeate produced. In addition to these, filtration needs to be carried out below the "critical flux" or at a "sustainable flux", at which no or little fouling occurs (Bacchin et al., 2006; Le-Clech et al., 2006). This limits the productivity in the sense that the permeate flow is kept at a low value. However, due to reduced fouling this value can be sustained for a longer time.

In submerged membrane bioreactors, where the membranes are immersed directly in the bioreactor, either flat sheet or hollow fiber membranes are used. Although the operation of flat sheet membranes is simpler due to better control over the hydrodynamics in the more well-defined geometry of the modules, hollow fiber membranes are less expensive to produce, backflushable and offer higher packing density (Cui et al., 2003; Judd, 2002). Increasing the membrane area per module volume can reduce the module production cost significantly and is highly desired (Buer and Cumin, 2010).

Recently we reported the fabrication of hollow fiber ultrafiltration membranes with a microstructured outer surface (Çulfaz et al., 2009). The membrane surface area in a given volume could be increased by up to 90%, and due to the increased area of the membranes' skin layer this was shown to increase the productivity of the fibers. In the present study, we report the performance of these microstructured hollow fibers in a submerged system with aeration, operated in different configurations, in comparison to round fibers with the same intrinsic properties.

2. Experimental

Microstructured and round hollow fiber membranes made by the dry–wet phase inversion of the polymer dope 16.68% PES, 4.91% PVP K30, 4.91% PVP K90, 7.18% H_2O, 66.32% NMP were used throughout this study. Details of the fabrication can be found elsewhere (Çulfaz et al., 2009). The outer perimeters of the structured fiber and round fiber were 7.5 mm and 4.7 mm, respectively, resulting in 60% higher surface area per volume for the structured fiber compared to the round fiber. The inner diameters of the structured and round fiber were 0.86 mm and 0.84 mm, respectively. The pure water permeability of the fibers are 235 ± 11 L/h m^2 bar and 233 ± 12 L/h m^2 bar for structured and round fibers, respectively. The mean pore diameter of both fibers was found to be 12 nm by permporometry.

The twisted membranes were made by twisting the structured fibers around their own axes, approximately one full turn per 10 cm. In the vertical module orientation, a steel tube was placed at the side of the fiber bundle to support the bundle. The fibers were fixed at the top and bottom ends and could move freely otherwise. The experimental setup, with drawings of both the vertical and horizontal module orientation is shown in Fig. 1. 4 and 7 fibers were used in vertical and horizontal modules, respectively. The module and fiber lengths were fixed for the structured, round and twisted membrane modules to provide the same degree of looseness and packing density. In vertical modules, the module length was 20 cm while the fiber length was 21 cm and in horizontal modules, the module length was 10.5 cm while the fiber length was 11 cm, providing 5% looseness for both kinds of modules (Wicaksana et al., 2006). Coarse bubbles were created by a perforated metal plate with 1 mm holes. Fine bubbles were created by a fritted ceramic plate with a nominal pore size of 0.1 mm.

The feed solution was 2 wt% Ludox-TMA colloidal silica (Sigma–Aldrich). The stock solution has 34 wt% silica in deionized water, with pH of 6–7.

2.1. *Flux-stepping experiments*

In the flux-stepping method used, the permeate fluxes were stepwise increased and then decreased back in the same steps while recording the transmembrane pressure difference (TMP). Each flux step was continued for 20 min. To be able to compare whether the convolutions in the structured fiber have an

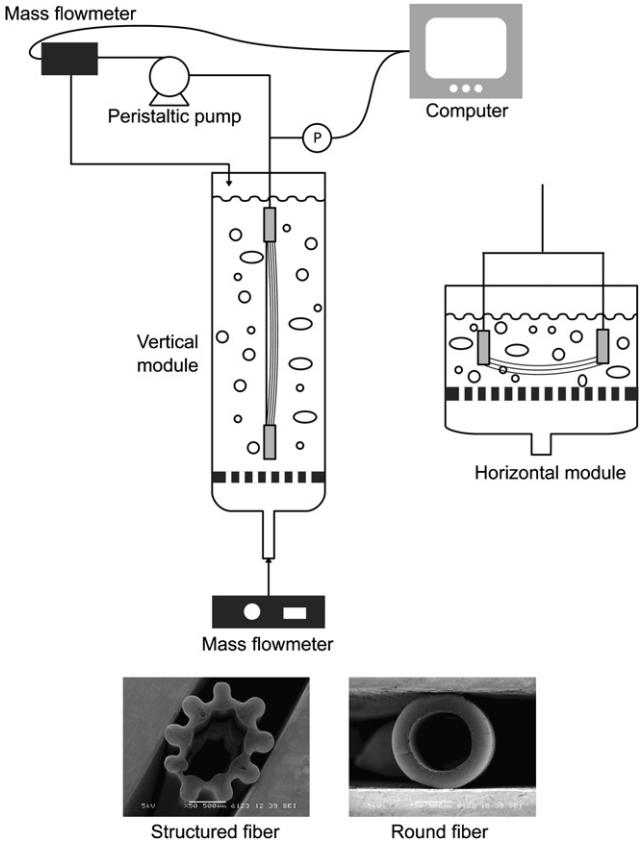

Fig. 1 – Experimental setup and the SEM images of the structured and round fibers.

improving effect on the hydrodynamics around the membrane, the permeate fluxes were set using the actual (convoluted, and therefore enhanced) surface area of the structured fibers. In the rest of the text, permeate flux refers to this flux calculated as the permeate flowrate through the actual surface area of the fibers. On the other hand, normalized permeate flux was calculated using the area of the circle passing through the middle of the fins for the structured fibers (Çulfaz et al., 2009). The latter is used to compare the fibers from a practical point of view, i.e. to compare the permeate volume that would be produced from the same module volume of round and structured fibers.

The fouling resistance was calculated using Darcy's law, expressing the total resistance during filtration as a resistance-in-series:

$$R_f = \frac{TMP}{\eta J_{per}} - R_m \quad (1)$$

where R_f is the fouling resistance which includes concentration polarization and/or particle deposition and R_m is the intrinsic membrane resistance determined by the pure water permeability.

3. Results and discussion

Fig. 2 shows the coarse and fine bubbles produced at different aeration rates. With the coarse bubbler, the bubbles formed had diverse size and shapes, from spherical to ellipsoid and cap-shaped. At 0.026 and 0.060 m^3/m^2 s, gas slugs were also observed. With the fine bubbler, only spherical or ellipsoid-shaped bubbles formed. At 0.002 m^3/m^2 s, the bubble size was between 0.3 and 4 mm, whereas at 0.008 m^3/m^2 s and 0.026 m^3/m^2 s, the bubble sizes were between 1 and 10 mm.

3.1. Comparison of round, structured and twisted fibers

Fig. 3 shows flux-stepping experiments with the structured and round fibers. A vertical module, coarse bubbles and an aeration rate of 0.008 m^3/m^2 s were used. At none of the fluxes, significant cake deposition was observed, which is indicated by a stable TMP at each flux, and equal TMP for a given flux both while stepping up and stepping down. However, the TMPs at each flux deviate from the pure water permeability values, indicating the presence of concentration polarization. This deviation is plotted for the round, structured and structured-twisted membranes in Fig. 4. Concentration polarization is highest in the structured fiber, less in the structured-twisted fiber and the lowest in the round fiber.

Bubbles prevent polarization and fouling through a number of different mechanisms. The scouring action of the bubbles on the membrane surface and the liquid mixing caused by the secondary flow in the bubble wakes are mechanisms effective in the pathway of the bubbles (Cui et al., 2003). Another factor that reduces particle deposition on the membrane is the fiber movement caused by the bubbles (Wicaksana et al., 2006; Yeo et al., 2007). Considering that the looseness of the fibers was similar for all three modules, this factor is not expected to create much difference between the fibers.

The higher concentration polarization on the structured fibers is related to the size of the bubbles in comparison to the size of the convolutions in the structured fibers. Since both the bubbles themselves and the wakes following the bubbles are much larger than the convolutions, the effect of the bubbles cannot reach the depths of the grooves, and leave stagnant areas more susceptible to concentration polarization and subsequent particle deposition. When the structured fibers were twisted, the polarization resistance is less than the structured fibers. In these twisted fibers, the convolutions are not parallel to the bubble trajectory as in the structured fibers. This can provide that more of the area within the grooves is within reach of the rising bubbles. Similarly, in another study where these fibers were used in cross-flow filtrations, less particle deposition was observed on twisted fibers compared to structured fibers (Çulfaz et al., submitted for publication). This was attributed to secondary flows which form due to the helical grooves and fins.

Fig. 5(a) shows the polarization resistances calculated using Equation (1) for the data in Fig. 4. In addition to the three modules in Fig. 4, in a fourth module (twisted-tight), the fibers were fixed more tightly, thus disabling much of the fiber movement cause by the bubbles. It was seen that the polarization resistance in this tight module was significantly higher than those of the loose modules. This supports previous observations showing that the looseness of the fibers is important in preventing fouling (Wicaksana et al., 2006; Yeo et al., 2007).

Considering that at a certain flux, the permeate production from the structured fibers is 60% more than the round fibers due to the enhanced surface area, the polarization resistances were also compared for the normalized fluxes, i.e. for equal amount of permeate production per fiber length or equivalently per module volume (Fig. 5(b)). From this figure it is seen that for the same permeate production, the structured and twisted fiber modules have lower polarization resistances than the round fibers.

3.2. Effect of aeration rate

Fig. 6 compares the polarization resistance at three aeration rates with coarse bubbles at a normalized flux of 70 L/h m^2. When the aeration rate is increased from 0.008 m^3/m^2 s to 0.026 m^3/m^2 s, the polarization resistance becomes less for the structured and round fibers, while it is not effected for twisted fibers. Increasing the aeration rate further to 0.060 m^3/m^2 s increases the resistance to higher values than for both of the other two aeration rates. It is often seen that there exists a critical aeration rate below which severe fouling occurs. Above this aeration rate there is little or no improvement in fouling performance (Ndinisa et al., 2006; Ueda et al., 1997). A high shear rate due to extensive aeration can also have detrimental effects, as it increases the shear-induced diffusion and inertial lift forces for the large particles and causes small particles, which can induce severe pore blocking and irreversible gel formation, to become the major foulants. The size of the silica particles used in our experiments is between 10 and 40 nm, which is small and narrow enough to exclude this effect due to increased shear. In our case, the negative effect of high aeration rate is probably due to decreased contact between the feed solution and the membrane because of the over-occupation of the reactor volume with the bubbles. Assuming that the bubbles reach a terminal velocity of 0.2 m/s

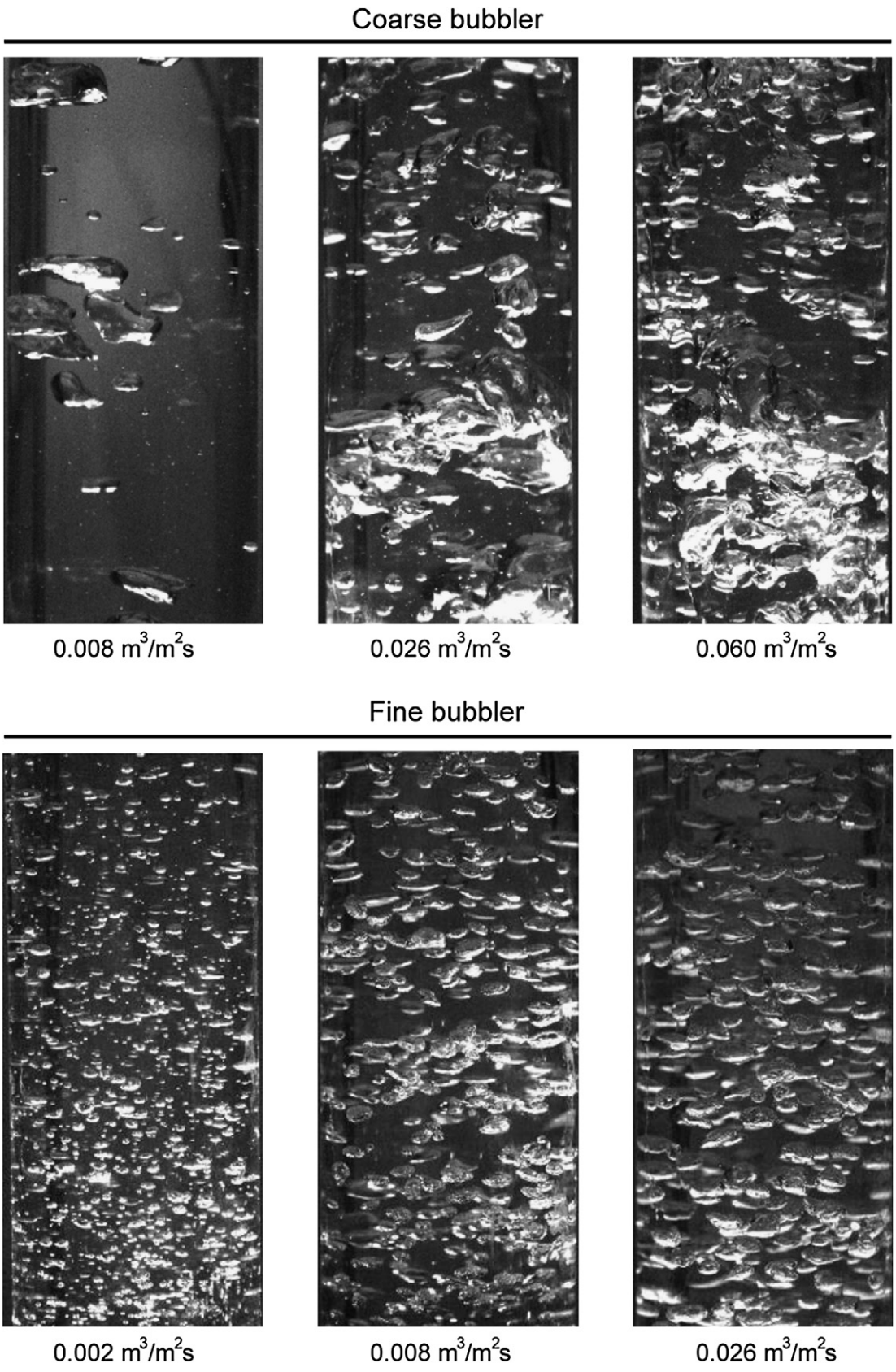

Fig. 2 – Bubbles produced by the coarse and fine bubblers at different aeration rates.

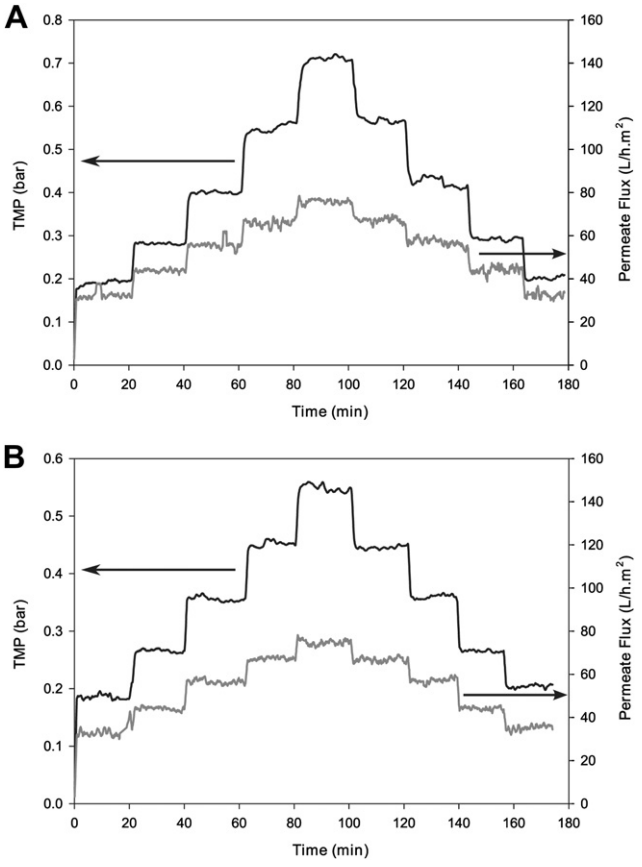

Fig. 3 – Flux-stepping experiments with (a) structured and (b) round fibers with vertical modules, large bubbles and an aeration rate of 0.008 m^3/m^2 s (0.8 L/min air flowrate).

(Fan and Tsuchiya, 1990), the residence time of a bubble in the reactor is estimated as 2 s. Then, with this aeration rate, the bubbles should occupy about 30% of the total reactor volume, which can cause such over-occupation.

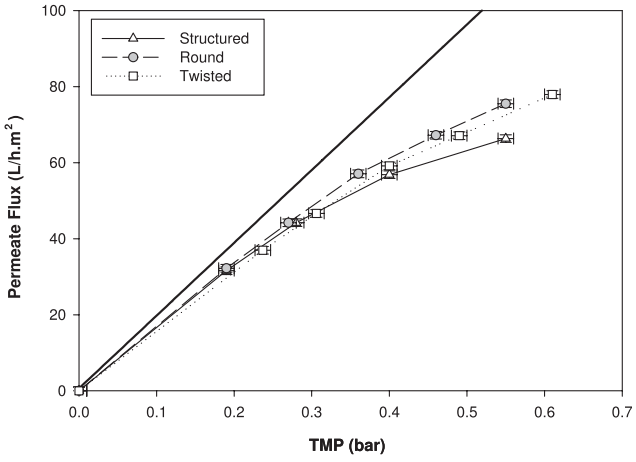

Fig. 4 – Pure water permeability of the membranes and the effect of concentration polarization causing deviation from pure water permeability. Vertical modules, large bubbles. Aeration rate: 0.008 m^3/m^2 s.

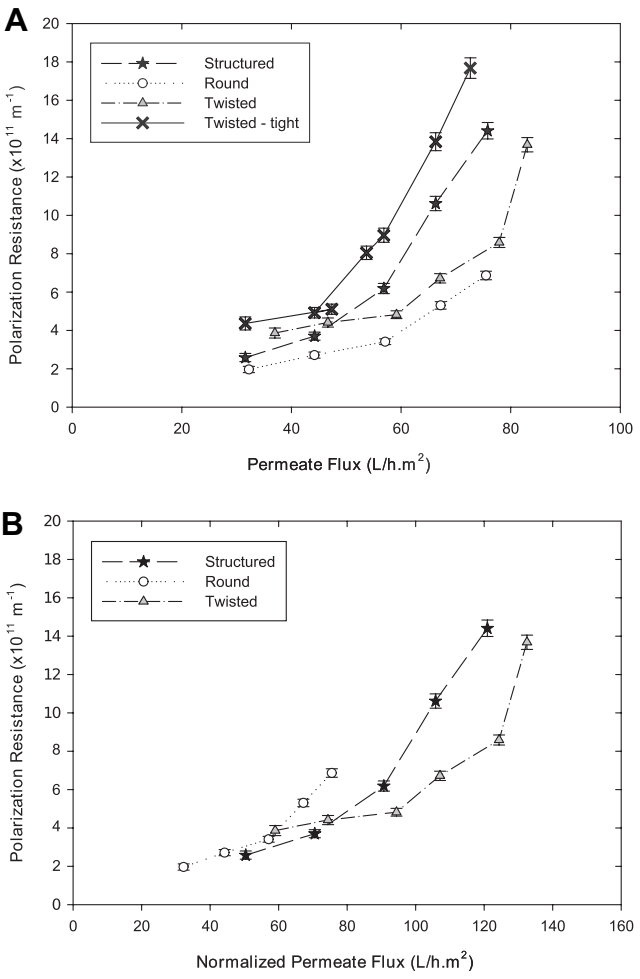

Fig. 5 – Polarization resistance as a function of permeate flux for four different types of membrane modules: Round, structured, twisted and twisted-tight. Vertical modules, large bubbles. Aeration rate: 0.008 m^3/m^2 s (0.8 L/min air flowrate). (a) Permeate flux is the flux through the actual (convoluted) membrane area for structured fibers. (b) Permeate flux is normalized by using the perimeter of a circle passing through the middle of the fins of the structured fiber, corresponding to a similar effective membrane volume as the round fibers.

3.3. *Effect of module orientation and bubble size*

Fig. 7 compares vertical and horizontal modules with large and small bubbles for an aeration rate of 0.026 m^3/m^2 s. When large bubbles were used, vertical modules performed significantly better than horizontal modules, as also reported by other researchers (Chang et al., 2002). In vertical modules, larger bubbles were more effective in depolarizing particle buildup than small bubbles. This higher depolarizing efficiency of large bubbles is attributed to the turbulent wake behind these cap-shaped bubbles and slugs (Cui et al., 2003).

With small bubbles the behavior was similar in vertical and horizontal modules. In a vertical module, the bubbles can sweep the complete surface of the fibers, whereas when the bubbles move perpendicular to the fiber bundle, dead zones occur at the

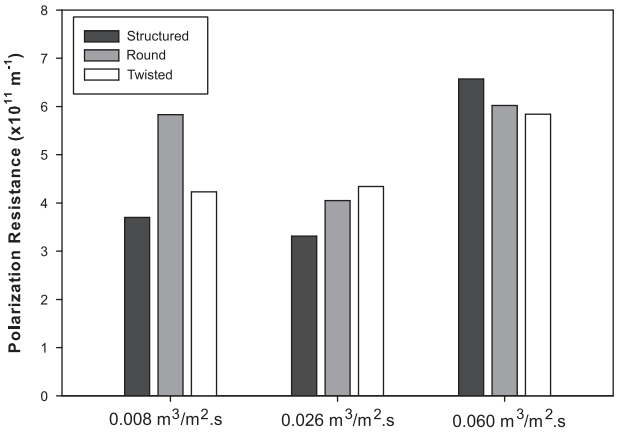

Fig. 6 – Polarization resistance at a normalized permeate flux of 70 L/h m^2 for round, structured and twisted membranes at different aeration intensities. Vertical modules, large bubbles.

back of the fiber bundle (Chang et al., 2002; Murai et al., 2005). Such dead zones are more likely to occur when large bubbles are used, since the size of these bubbles (5–20 mm) is larger than the spacings between individual fibers in the bundle. In this case, the bubbles would preferentially sweep through the periphery of the module and not penetrate through the bundle, leaving the fibers in the inner parts of the bundle as well as the back of the fiber bundle more susceptible to polarization and fouling. For small bubbles (1–10 mm), at least part of the bubbles can penetrate between the fiber bundle, causing mixing and preventing polarization in an equivalent manner to vertical modules.

3.4. *Effect of sub-mm sized bubbles*

As shown in Fig. 2, the bubble size was dependent on both the sparger used and the air flowrate. Using a fine bubbler and a low aeration rate of 0.002 m^3/m^2 s, bubbles of sizes close to the size of the corrugations of the structured fibers could be formed. It was observed that the polarization resistances under these conditions were much higher than those for higher aeration rates used with the same bubbler (Fig. 8). Furthermore, at the highest fluxes indicated for each fiber, cake deposition started to occur, observed as an increasing TMP during the constant flux filtration. Under these conditions, although the size of the bubbles was on the order of the size of the convolutions in the structured fiber, the bubbles did not cause any enhancement in preventing polarization in these fibers. If the bubbles would have been able to reach within the grooves in the structured fibers, we would see at least a comparable resistance in the structured and round fibers. However, the resistance in the structured fibers is much higher than that of the round fiber. Yeo et al. reported that small bubbles (0.11 cm^3 which corresponds to about 6 mm diameter in their experiments) seldom moved close to the fibers (Yeo et al., 2007). In addition to this, it has been shown that in a submerged membrane operation, the secondary flows caused by the bubbles are at least as effective as the scouring action of the bubbles themselves in fouling prevention (Cui et al., 2003; Le-Clech et al., 2006). Around bubbles smaller than 1 mm, there are no wake structures, and therefore no secondary flows and mixing. Instead there are laminar streamlines, which can only be as effective as liquid cross flow over the membrane.

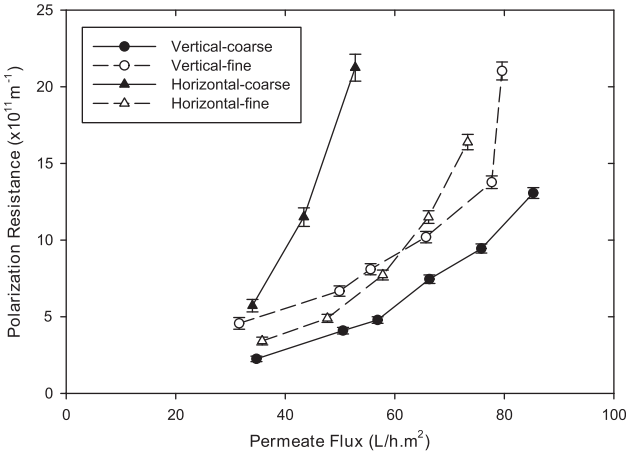

Fig. 7 – Polarization resistance as a function of permeate flux for vertical and horizontal membrane modules, large and small bubbles for the structured membrane. Aeration rate: 0.026 m^3/m^2 s.

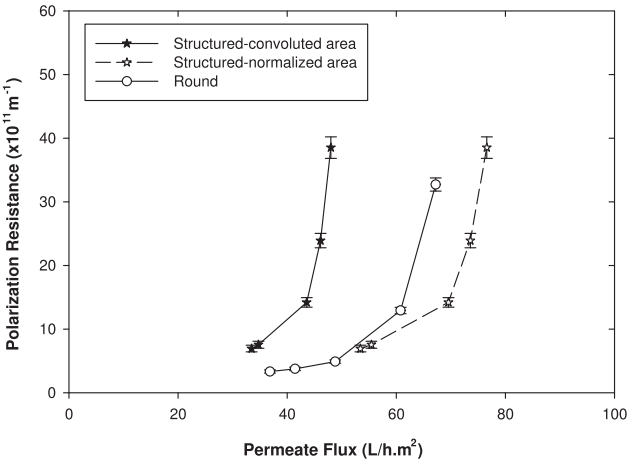

Fig. 8 – Polarization resistance as a function of permeate flux for small bubbles of 0.3–4 mm produced at an aeration rate of 0.002 m^3/m^2 s. Vertical modules.

4. Conclusions

The performance of microstructured hollow fiber membranes in a submerged and aerated system was investigated using colloidal silica as a model foulant. The fouling in structured fibers was found to be less than round fibers for the same permeate production per module volume. However, when the fibers were compared at the actual permeate flux through the convoluted area of the structured fibers, the fouling resistance in the structured fibers were higher.

When large bubbles were used, since bubble size was much larger than the convolutions, the bubbles and secondary flows they create were not able to reach the whole area of the structured fibers. This created stagnant areas in the grooves, which results in a higher overall resistance. On the other hand, bubbles of sizes similar to the groove dimensions also did not improve the fouling performance in the structured fibers. In general, large, cap-shaped bubbles and slugs were found to be the most effective in fouling removal, as they produce more turbulent wakes behind them and induce more fiber movement.

Twisting the structured fibers around their axes decreased the fouling resistance, since by twisting, more of the area within the grooves became within reach of the bubbles passing by.

Modules in a vertical orientation performed better than horizontal modules when coarse bubbles were used. On the other hand, for small bubbles, vertical and horizontal modules showed similar fouling behavior.

In general, the structured fibers, in their original straight form or as twisted around their own axes, did not cause further enhancement in liquid mixing in the aerated systems. Furthermore, in most of the cases, due to stagnant zones remaining within the grooves, the fouling resistance was higher for these fibers. However, under the low-fouling conditions used in the present study, the increase in fouling resistance for the structured and twisted fibers was lower compared to the surface area enhancement due to the microstructured surface. This implies that in submerged, aerated systems structured fibers can still offer enhanced productivity per module volume for the same permeate production compared to round fibers.

REFERENCES

Bacchin, P., Aimar, P., Field, R., 2006. Critical and sustainable fluxes: theory, experiments and applications. Journal of Membrane Science 281, 42–69.

Buer, T., Cumin, J., 2010. MBR module design and operation. Desalination 250, 1073–1077.

Çulfaz, P., Haddad, M., Wessling, M., Lammertink, R. Fouling behavior of microstructured hollow fibers in cross-flow filtrations: critical flux determination and direct visual observation of particle deposition. Journal of Membrane Science, submitted for publication.

Çulfaz, P., Rolevink, E., van Rijn, C., Lammertink, R., Wessling, M., 2009. Microstructured hollow fibers for ultrafiltration. Journal of Membrane Science 347, 32–41.

Chang, S., Fane, A., Vigneswaran, S., 2002. Experimental assessment of filtration of biomass with transverse and axial fibres. Chemical Engineering Journal 87, 121–127.

Cui, Z., Chang, S., Fane, A., 2003. The use of gas bubbling to enhance membrane processes. Journal of Membrane Science 221, 1–35.

Fan, L., Tsuchiya, K., 1990. Bubble Wake Dynamics in Liquids and Liquid–Solid Suspensions. Butterworth.

Ho, C.C., Zydney, A., 2006. Overview of fouling phenomena and modeling approaches for membrane bioreactors. Separation Science and Technology 41, 1231–1251.

Judd, S., 2002. Submerged membrane bioreactors: flat plate or hollow fibre? Filtration and Separation 39, 30–31.

Judd, S., 2008. The status of membrane bioreactor technology. Trends in Biotechnology 26, 109–116.

Le-Clech, P., Chen, V., Fane, T., 2006. Fouling in membrane bioreactors used in wastewater treatment. Journal of Membrane Science 284, 17–53.

Melin, T., Jefferson, B., Bixio, D., Thoeye, C., De Wilde, W., De Koning, J., van der Graaf, J., Wintgens, T., 2006. Membrane bioreactor technology for wastewater treatment and reuse. Desalination 187, 271–282.

Meng, F., Chae, S.R., Drews, A., Kraume, M., Shin, H.S., Yang, F., 2009. Recent advances in membrane bioreactors (MBRs): membrane fouling and membrane material. Water Research 43, 1489–1512.

Murai, Y., Sasaki, T., Ishikawa, M.A., Yamamoto, F., 2005. Bubble-driven convection around cylinders confined in a channel. Journal of Fluids Engineering, Transactions of the ASME 127, 117–123.

Ndinisa, N., Fane, A., Wiley, D., 2006. Fouling control in a submerged flat sheet membrane system: Part i - bubbling and hydrodynamic effects. Separation Science and Technology 41, 1383–1409.

Shannon, M., Bohn, P., Elimelech, M., Georgiadis, J., Maras, B., Mayes, A., 2008. Science and technology for water purification in the coming decades. Nature 452, 301–310.

Sofia, A., Ng, W., Ong, S., 2004. Engineering design approaches for minimum fouling in submerged mbr. Desalination 160, 67–74.

Ueda, T., Hata, K., Kikuoka, Y., Seino, O., 1997. Effects of aeration on suction pressure in a submerged membrane bioreactor. Water Research 31, 489–494.

Wicaksana, F., Fane, A., Chen, V., 2006. Fibre movement induced by bubbling using submerged hollow fibre membranes. Journal of Membrane Science 271, 186–195.

Yeo, A., Law, A., Fane, A., 2007. The relationship between performance of submerged hollow fibers and bubble-induced phenomena examined by particle image velocimetry. Journal of Membrane Science 304, 125–137.